Macromol. Symp. **2016**, 363, 36–48

DOI: 10.1002/masy.201500145

Physicochemical Properties of Hydrophobically Modified Polymeric Betaines and of Their Langmuir-Blodgett Films

Evgeniya V. Seliverstova,[1] Niyaz Kh. Ibrayev,[1] Alexey V. Shakhvorostov,[2,3] Nurxat Nuraje,[4,5] Sarkyt E. Kudaibergenov[2,3]*

Summary: Polymeric betaines containing long alkyl chains ($C_{12}H_{25}$, $C_{13}H_{27}$, $C_{14}H_{29}$, $C_{16}H_{33}$ and $C_{18}H_{37}$) were synthesized by Michael addition reaction of alkylaminocrotonates and methacrylic acid. They were characterized by FTIR, ^{13}C NMR, DLS, TEM, viscometry and zeta-potential measurements. In aqueous KOH and DMSO solutions the hydrophobically modified polymeric betaines behave polyelectrolyte character. The average hydrodynamic size and zeta potential of diluted aqueous solutions of hydrophobic polybetaines containing tetradecyl- and octadecyl groups were studied as a function of pH. Anomalous low values of the isoelectric point (IEP) of amphoteric macromolecules were found to be in the range of pH 2.7–3.4. The TEM results revealed that in both aqueous KOH and DMSO media the nano- and microsized micelles and vesicles are existed. The structural organization of micelles and vesicles in water and water – DMSO mixture is discussed. Langmuir-Blodgett (LB) monolayers on the water-air interface were obtained by spreading of hydrophobic polybetaines containing tetradecyl- and octadecyl groups dissolved in THF on the subphase surface. The LB films on the subphase surface are characterized by the specific areas of $0.6 \pm 0.05\ \text{nm}^2 \cdot \text{monomeric unit}^{-1}$ at collapsed state. In the spectra of Langmuir-Blodgett film the absorption band with the maximum at 255 and 270 nm was observed.

Keywords: amphihiles; isoelectric point; LB films; micellar and vesicular structures; polymeric betaines

Introduction

The hydrophobic polyampholytes (HPA) are unique class of macromolecules containing both ionizable and hydrophobic moieties in the main (or side) chain.[1–3] The structure, morphology, hydrodynamic and conformational properties of HPA depend on phase conditions (solid or liquid) and the influence of external factors such as pH, ionic strength, temperature, water-organic solvents etc. Two main concurring forces – electrostatic repulsion (or attraction) and hydrophobic interactions – are responsible for existing of macromolecules in amorphous, ordered, expanded, coiled and globular states. The specific properties of HPA are competition of "antipolyelelctrolyte" (expanding of macromolecular chain) and hydrophobic effects (aggregation) upon addition of salts. One of the most interesting solution properties of HPA described by authors[4,5] is their ability to self-assemble into

---

[1] Institute of Molecular Nanophotonics, Y.A. Buketov Karaganda State University, Universitetskaya str. 28, Karaganda, Kazakhstan
E-mail: genia_sv@mail.ru

[2] Laboratory of Engineering Profile, Kazakh National Technical University n/a, K.I. Satpayev, Satpaev str. 22, Almaty, Kazakhstan

[3] Institute of Polymer Materials and Technology, Satpayev str. 22, Almaty, Kazakhstan

[4] Department of Chemical Engineering, Texas Tech University, 6th Str. and Canton Ave., Lubbock, TX 79409-3121, USA

[5] Department of Materials Science and Engineering, Massachusetts Institute of Technology, Massachusetts Ave. 77, Cambridge, MA 02139-4307, USA

"schizophrenic" micelles, lamellar aggregate, vesicles and hydrogels.

The literature survey reveals that the HPA are less studied subject in comparison with ordinary polyampholytes composed of only acidic and basic groups. There is a considerable interest in the adsorption of both natural and synthetic polyampholytes at the air–liquid, liquid/liquid and solid/liquid interfaces because many of biological and technological processes are closely connected with adsorption phenomenon.[6] The understanding of adsorption and desorption of polyampholytes is fundamental for medicine, biotechnology, membrane technology, photography, cosmetic, waste water and sludge treatment, etc.

Stimuli responsive amphiphilic macromolecules are the most promising class of polymers to be used for design of polymeric membranes and for application in water treatment, food manufacturing, purification of proteins and biomedicine.[7,9–11] It was shown[10,12,13] that coupling of hydrophobic species to polybetaines prevents excessive adsorption of protein molecules and microorganisms to polymeric molecules. This effect is achieved due to hydrophilic nature of biofouling.[8] In addition, hydrophobically modified polymers could be useful for preparation of unwettable films that are used in optics and technics. [14,15]

Langmuir-Blodgett (LB) technique is powerful tool that permits to form functional polymer coatings with predicted properties.[16] This technology allows the formation of ordered layers of amphiphilic macromolecules on the surface of the liquid subphase and transferring of monolayers onto solid substrates. Despite the fact that the LB method is widely used to create a lipid-based membrane and protein compounds,[17,18] the researches on using of this method for forming of polybetaine monolayers and studying of their physicochemical properties, are restricted. For example, LB films of poly(N,N-diallyl-N-octadecylamine-alt-maleic acid) as well as mixed films consisting of hydrophobic polyampholyte and two amphiphilic fluorophores – alkyl substituted rhodamine dyes – were prepared and investigated.[19,20] The preparation and characterization of polymeric betaines based on aminocrotonates was reviewed in[21] where the stereochemistry and tautomeric transitions as well as kinetics and mechanism of formation of linear and crosslinked polybetaines proceeding via Michael addition reaction were outlined.

As continuation of our previous studies[19–22] in the present paper we describe the synthetic protocol of the hydrophobically modified polymeric betaines. The influence of external factors on the structure and properties of hydrophobic polyampholytes was shown and the phase state of polybetaine monolayers on the water–air interface including the condition of transfer of monolayer onto solid substrate was evaluated. The obtained results can serve as a basis for design of membranes and coatings with predicted structure and behavior.

Experimental Section

Materials

Acetoacetic ester (ethyl acetoacetate) (99%), dodecylamine (99%), tridecylamine (99%), tetradecylamine (99%), hexadecylamine (99%), octadecylamine (99%), methacrylic acid (99%), and azoisobutyronitrile (AIBN) were purchased from Aldrich. Methacrylic acids was purified by distillation under the low pressure and kept in refrigerator. Reagent grade solvents acetone, DMF, THF and DMSO purchased from Aldrich were used.

Methods

NMR ^{13}C spectra of polymer samples in DMSO were registered on impulse Fourier NMR spectrometer Bruker 400 MHz (Bruker, Germany). UV and FTIR spectra were recorded with the help of Cary 300 and Carry 660 (Agilent, USA) respectively.

The average hydrodynamic size and zeta-potential of colloid particles was determined by dynamic light-scattering technique with the help of Malvern Zetasizer Nano ZS90 (UK) at room temperature.

The TEM measurements were carried out on JEOL JEM-2100 instrument. The viscosity of polymer solutions was measured by Ubbelohde viscometer at $25 \pm 0.1\ ^\circ C$.

Behavior of monolayers was studied on Langmuir-Blodgett (LB) trough by measuring the dependence of surface pressure-specific molecular area (π-A–isotherm). The automatized Langmuir device with active area of 396 cm^2 and volume of 1.5 L was assembled at the Russian State Scientific Centre "NIOPIK" (Moscow).[20] Surface pressure at the air – water interface was registered with the help of a Wilhelmy balance. The compression rate of the monolayers in the course of measuring of π–A isotherm and transferring of monolayer onto solid substrates from quartz glass was $2\,mm \cdot min^{-1}$. The deionized water was cleaned by AquaMax and was used as subphase. The resistivity of the deionized water was equal to $18.2\,M\Omega \cdot cm$ with the surface tension of $72.8\,mN \cdot m^{-1}$ at pH = 5.6 and temperature 22 °C. The monolayers were deposited by spreading of polymer solution in THF onto water surface. The concentration of polymer was equal to $0.15\,mg\,L^{-1}$. It is known that more volatile solvents such as benzene, chloroform and hexane[16,23] are usually used for monolayer formation. However it was found that synthesized polybetaines are insoluble in above mentioned solvents. Additional experiments show that surface pressure is equal to $0.5\,mN \cdot m^{-1}$ after 30 min solution spreading onto subphase surface. In addition, the density of THF is less than density of water. It means that, despite the fact that the THF is miscible with water, it does not form a saturated solution[16] and causes no noticeable effect on the surface properties of the polymer monolayers due to the large area and volume of used subphase.

Monolayers were transferred onto quartz substrates by vertical dipping according to Y-type transfer (transfer during downward and upward stroke) at constant pressure and rate equal to $5\,mm \cdot min^{-1}$. The number of layers in LB films was equal to 4.

Monomer Synthesis

Preliminary melted alkylamines were dropwise added to acetoacetic ester (AAE) under the stirring during 3 h at 60 °C. The reaction mixture was left overnight at room temperature. Table 1 demonstrates the synthetic protocol of alkylaminocrotonates including the yield of abbreviated key products.

Interaction of AAE with alkylamines proceeds by Scheme 1. Alkylamino-but-2-enoic acid ethyl esters are more energetically stable than the alternative tautomeric forms – 3-alkylamino-butyric acid ethyl esters due to conjugation of C=C and C=O bonds and formation of intramolecular hydrogen bonds.[21,22]

Polymer Synthesis

Polymerization of alkylaminocrotonates and MAA was carried out in benzene at 70 °C in the presence of AIBN. Addition of methacrylic acid to alkylaminocrotonates leads to formation of betaine monomers

Table 1.
The synthetic protocol of alkylaminocrotonates from AAE and alkylamines.

Alkylamines	Number of carbon atoms	The mass of alkylamine [g]	The mass of AAE [g]	Reaction temperature [°C]	Yield of product [%]	Abbreviation of monomers
Dodecylamine	12	10	7.02	60	>95	CRODDA
Tetradecylamine	14	10	6.10	60	>95	CROTDA
Hexadecylamine	16	10	5.39	60	>95	CROHDA
Octadecylamine	18	10	4.83	60	>95	CROODA

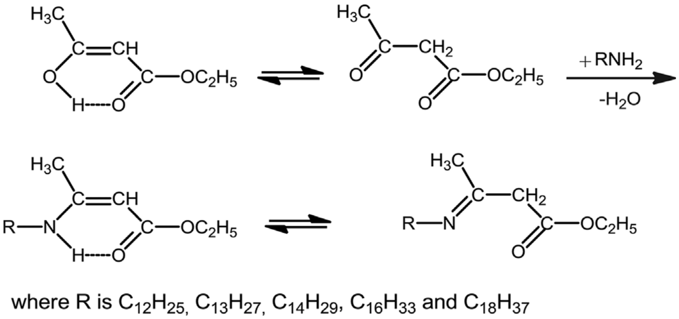

Scheme 1.
Formation of alkylaminocrotonates from AAE and alkylamines.

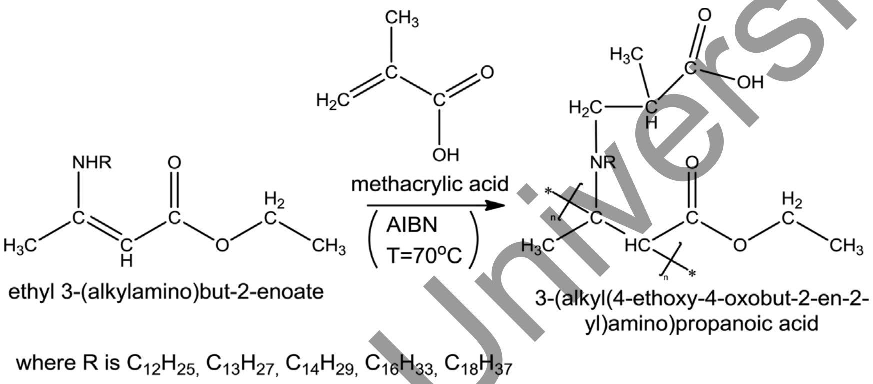

Scheme 2.
Polymerization of alkylaminocrotonates in the presence of MAA.

which undergo radical polymerization in the presence of AIBN (Scheme 2).

The monomer mixture was bubbled by nitrogen gas during 15 min, sealed into ampoule and thermostated at 70 °C during 5 h. After completion of polymerization reaction, the precipitated product was washed out by acetone several times and dried at 70 °C in vacuum oven up to constant mass. Table 2 represents the synthetic conditions of alkylaminocrotonates.

The radical polymerization of 3-[(2-carboxypropyl)alkylamino]-but-2-enoic acid ethyl ester leads to formation of hydrophobically modified linear polybetaines abbreviated as CRODDA-MAA, CROTriDA, CROTDA-MAA, CROHDA-MAA and CROODA-MAA respectively in dependence of alkyl chain length.

Table 2.
Synthetic protocol of hydrophobically modified polymeric betaines.

Alkylaminocrotonate					
Abbreviation	Mass [g]	Amount of MAA [g]	AIBN, mg [g]	T [°C]	Yield of product [%]
CRODDA	7	2.03	0.02667	70	~50
CROTDA		1.85			~45
CROHDA		1.70			~43
CROODA		1.58			~39

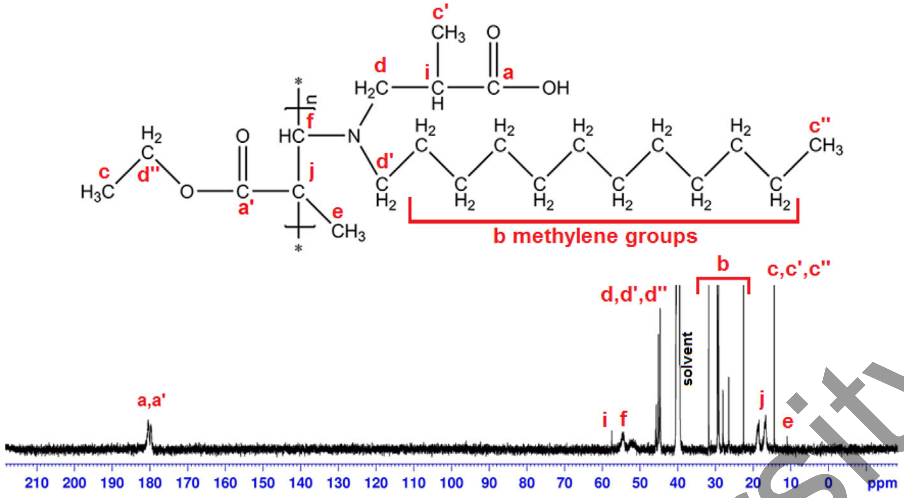

Figure 1.
NMR ^{13}C spectra of CRODDA-MAA in DMSO.

Results and Discussion

NMR ^{13}C Spectra of Polymers

The structural unit and ^{13}C NMR spectra of CRODDA-MAA together with identification of functional groups are shown in Figure 1.

The^{13}CNMR spectra of CROTDA-MAA, CROHDA-MAA and CROODA-MAA are similar to CRODDA-MAA and differs each other only by additional methylene groups.

FTIR Spectra of Monomers and Polymers

Identification of FTIR spectra of monomers and polymers is given in Tables 3 and 4.

Viscosity

The viscosity of CROTDA and CROODA upon dilution was measured in aqueous KOH and DMSO solutions. In both aqueous KOH and DMSO the reduced viscosity gradually increases with dilution demonstrating the polyelectrolyte behavior of polymers. The viscosity of CROTDA and CROODA in aqueous KOH is high because the carboxylic groups of polymeric betaines are in ionized state and effectively unfold the macromolecular chains. The lower viscosity of CROTDA and CROODA in DMSO may be connected with lower dielectric constant of organic solvent that retards the Coulomb repulsion of charged macromolecules.

Table 3.
Identification of FTIR spectra of alkylaminocrotonate monomers.

	Wavenumber [cm^{-1}]			
Functional groups	CRODDA	CROTDA	CROHDA	CROODA
$\nu(CH)_{as}$	2923 (vs)	2918 (vs)	2925 (vs)	2922 (vs)
$\nu(CH)_{s}$	2853 (s)	2849 (s)	2855 (s)	2850 (s)
$\nu(C=O)$	1652 (vs)	1649 (vs)	1651 (vs)	1650 (vs)
$\nu(C=C)$	1610 (vw)	1604 (vw)	1608 (vw)	1605 (vw)
$\nu(COC)$	1099 (w)	1096 (w)	1095 (w)	1099 (w)

Band intensities and vibration types: vs, very strong; s, strong; w, weak; vw, very weak; s, symmetric; as, asymmetric.

Table 4.
Identification of FTIR spectra of CRODDA-MAA, CROTriDA-MAA, CROTDA-MAA, CROHDA-MAA and CROODA-MAA.

	Wavenumber [cm^{-1}]				
Functional groups	CRODDA-MAA	CROTriDA-MAA	CROTDA-MAA	CROHDA-MAA	CROODA-MAA
ν (OH)	3402	3422	3422	3420	3419
ν $(CH)_{as}$	2929 (s)	2927 (s)	2927 (s)	2928 (s)	2926 (s)
ν $(CH)_{s}$	2856 (s)	2855 (s)	2855 (s)	2856 (s)	2854 (s)
ν (C = O)	1701 (vs)	1703 (vs)	1703 (vs)	1704 (vs)	1703 (vs)
ν $(COO^{-})_{as}$	1541 (m)	1542 (m)	1542 (m)	1541 (m)	1542 (m)
ν $(COC)_{as}$	1182 (s)	1183 (s)	1183 (s)	1181 (s)	1182 (s)

Band intensities and vibration types: vs, very strong; s, strong; m, moderate; w, weak; vw, very weak; s, symmetric; as – asymmetric.

The Average Hydrodynamic Size and Zeta-Potential of Hydrophobic Polymers

The average hydrodynamic size and zeta-potential of CROTDA-MAA, CROTriDA and CROODA-MAA measured in dilute aqueous KOH solutions are summarized in Table 5. The average hydrodynamic size of macromolecules tends to increase with increasing the polymer concentration due to formation of bigger aggregates stabilized by hydrophobic interactions. In DMSO such tendency is also observed because of formation of ionic associates. Extremely big aggregates in DMSO are characteristic for CROODA-MAA that has a long alkyl chains. Zeta-potential of macromolecules in both aqueous KOH and DMSO is negative due to ionization of carboxylic groups. Much lower zeta-potential of macromolecules in DMSO is probably connected with the low dielectric permittivity of organic solvent ($\varepsilon = 39.5$) leading to enhancement of charge compensation between positive and negative charges of betaine groups.

pH Dependent Average Hydrodynamic Size and Zeta Potential of Diluted Aqueous Solutions of CROTriDA, CROTDA-MAA and CROODA-MAA

According to zeta-potential measurement, the isoelectric point (IEP) of 0.01% aqueous solution of CROTDA-MAA corresponds to pH 3.4. At the same time the minimal size of CROTDA-MAA obtained from the DLS data is around of pH 2.5 (Figure 2a).

Such inconsistency may be attributed to fluctuation of the size of macromolecules near of the IEP and experimental errors in

Table 5.
The average hydrodynamic size and zeta-potential of CROTriDA-MAA, CROTDA-MAA and CROODA-MAA in aqueous KOH and DMSO.

		The average hydrodynamic size [nm]		Zeta-potential [mV]	
Polymer	Concentration [g · dL^{-1}]	Aqueous KOH	DMSO	Aqueous KOH	DMSO
CROTriDA-MAA	0.05	–	–	−18	–
	0.10	11.6	–	−19.2	–
	0.20	4.8	–	−15	–
	0.30	7.8	–	−18.7	–
CROTDA-MAA	0.05	258	–	−48.7	−4.3
	0.10	306	338	−60.0	−7.6
	0.20	316	411	−47.7	−8.2
	0.30	1576	429	−30.1	−5.4
CROODA-MAA	0.05	237	594	−47.8	−7.7
	0.10	253	2600	−45.5	−6.5
	0.20	487	5333	−42.3	−4.6
	0.30	1789	5560	−37.0	−3.5

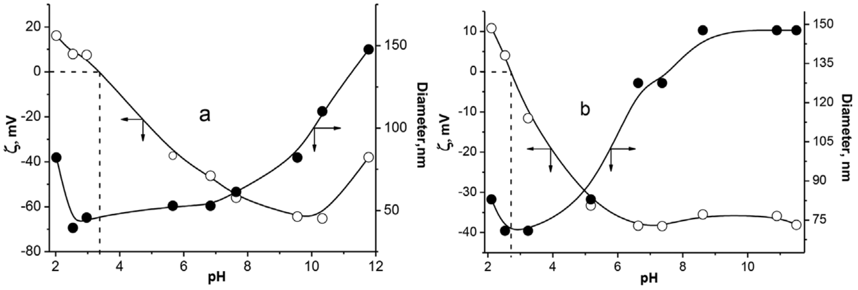

Figure 2.
The dependences of the average hydrodynamic size and zeta-potential of CROTDA-MAA (a) and CROODA-MAA (b) as a function of pH.

case of DLS measurements. The IEP of 0.01% aqueous solution of CROODA-MAA according to zeta potential measurement corresponds to pH 2.7. This value is in good agreement with DLS data ($pH_{IEP} \approx 2.9$) (Figure 2b). The value IEP of CROTriDA-MAA found from the viscosity and DLS data is in the interval of 2.7–2.9. Earlier the anomaly low values of the IEP (pH 2–2.1) was observed for poly(carboxyethyl 3-aminocrotonate).[22] The average hydrodynamic sizes of dilute aqueous solution of CROTriDA-MAA, CROTDA-MAA and CROODA-MAA in dependence on pH are varied in the range of 40–350 nm, 40–150 nm and 70–150 nm respectively. The increase of the average diameter of CROTDA-MAA and CROODA-MAA at high pH is due to ionization of carboxylic groups that leads to electrostatic repulsion between macroions and consequently to expanding of macromolecules. A slight increase of the average diameter is observed at $pH \approx 2$ due to protonation of nitrogen atoms. Carboxylic groups disposed far from the main chain can be ionized more easily than the secondary amine groups that are near the main chain and in a hydrophobic environment. Therefore, ionization of carboxylic groups more effectively unfolds the macromolecules than the ionization of nitrogen atoms located close to the main chain.

TEM Measurements

Polymeric micelles can be represented as self-assembled, nano- or microsized colloidal particles which form spontaneously in an aqueous environment to minimize the contact of the hydrophobic segment with the aqueous media, leading to the formation of a *core-shell* micellar structure.[24,25] In aqueous KOH solution the carboxylic groups are in ionized state and responsible for polyelectrolyte behavior. According to commonly accepted approach, the hydrophobic groups in aqueous solution will tend to form intramacromolecular micelle or inter-macromolecular vesicular structures stabilized by hydrophobic interactions of long alkyl groups as shown in Figure 3. The existence of such structures is good seen from TEM measurements.

The morphologies of CROHDA-MAA and CROTDA evaporated from aqueous KOH solutions are represented in Figure 4. According to TEM results, the colloidal particles have uniformed (or regular) spherical or toroidal-shaped forms. The size of uniformed micelles (Figure 4a) is about 100 nm, while the outer diameter of toroidal-shaped micelle is 150 nm with its internal diameter 40 nm. The inner part of uniformed micelle structure (Figure 4a,c) seems fully represented by long alkyl chains, while the hole part of toroid-shaped micelle (Figure 4b,d) probably contains the structured or “iceberg-like” water molecules surrounded by hydrophobic environment. Schematically the structure of uniformed spherical micelle and toroidal-shaped micelle structures are shown in Figure 5c,d.

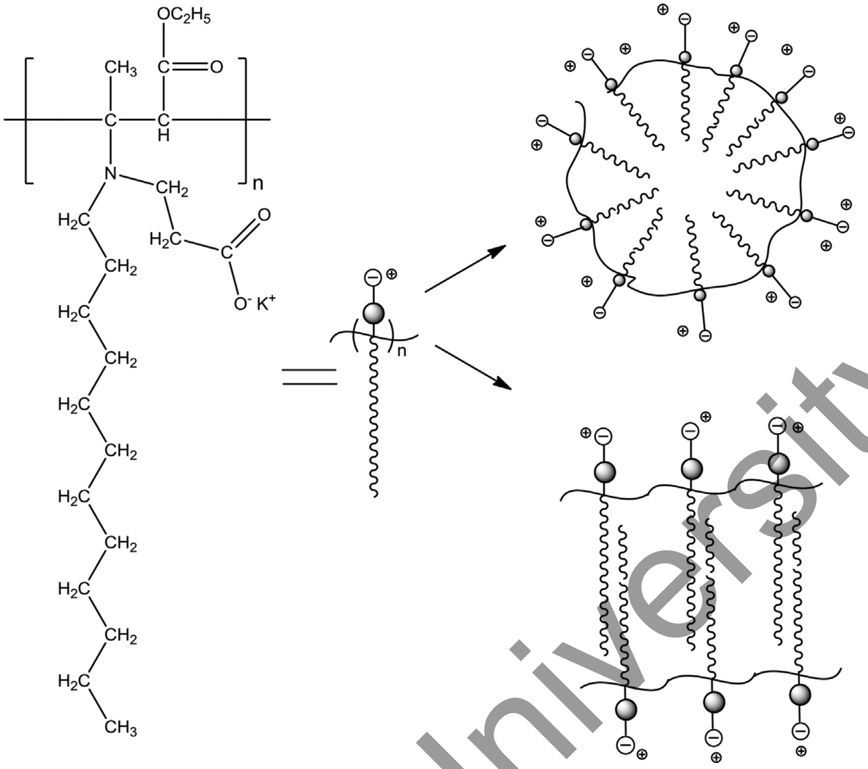

Figure 3.
Schematic representation of formation of micellar and vesicular structures of hydrophobic polybetaines in aqueous KOH solutions.

Schematically the structure of uniformed spherical micelle and toroidal-shaped micelle structures are shown in Figure 4c,d. Due to existence of hydrophobic "tail" and hydrophilic "head" in macromolecules, they are able to self-assembling into tubular vesicles with the length about 200–300 nm and average diameter around 20–30 nm (Figure 5a–c). Such vesicles are probably the result of association of several inter-macromolecular chains stabilized by hydrophobic interactions. Also the formation or rod-like micelles with large length-to-diameter aspect ratios was observed (Figure 5d).

The DLS measurements (Table 5) are satisfactorily correlated with TEM observations (Figure 6), e.g. the hydrodynamic radius measured by DLS is close to the size of the nano- and microparticles seen via TEM. The self-assembled aggregates of hydrophobically betaine type polyampholytes have potential utilizations in mimicking biological tubular structures or in drug delivery systems. In contrast to aqueous KOH solution the morphology of hydrophobic polyampholyte in organic solvent – DMSO is different. As seen from Figure 6 the existence of uniformed nanosized micelles is also observed in DMSO.

They represent either expelled spherical particles with various diameters (100–300 nm) or bigger aggregates (d = 300 nm) consisting of smaller nanoparticles with d = 10–15 nm. It is suggested that within such aggregates exist both "direct" and "reverse" or mixed micelles. It is supposed that in DMSO some parts of ionized groups tend to be replaced inside

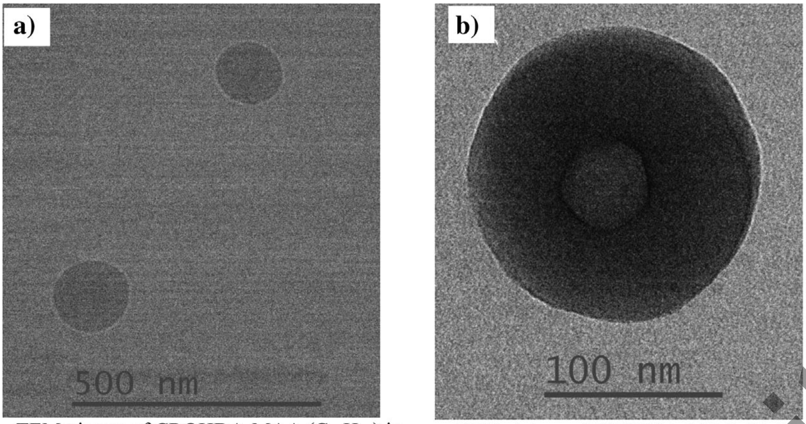

TEM picture of CROHDA-MAA ($C_{16}H_{31}$) in aqueous KOH. C=15 mg/mL

TEM picture of CROTDA-MAA ($C_{14}H_{29}$) in aqueous KOH. C=45 mg/mL

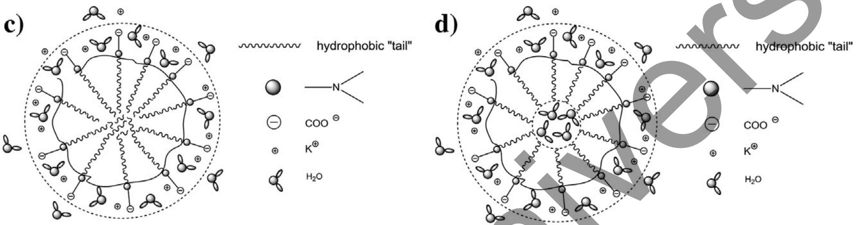

Schematic representation of micelle structure stabilized by hydrophobic association of long alkyl chains

Schematic representation of toroidal-shaped structure stabilized by hydrophobic association of long alkyl chains

Figure 4.
TEM pictures of CROHDA-MAA (a) and CROTDA-MAA (b) in aqueous KOH solution at concentrations of 15 (a) and 30 mg/mL (b) and the schematic representation of micelle (c) and toroidal-shaped (d) particles.

of micelle due to less solubilization in organic solvent while the most hydrophobic parts are replaced in corona due to good solubility in DMSO.

The Physico-Chemical Properties of CROTDA-MAA and CROODA-MAA Monolayers

Study of physico-chemical properties of monolayers on the surfaces is traditional method for investigation of interaction of molecules within the monolayer and with the subphase. Comprehensive information on the phase state of monolayers can be obtained from the dependence of surface pressure (π) on the specific molecular area (A) within the monolayer (π-A–isotherms). Phase state is attributed to degree of freedom of molecules in the monolayer under its compression. Phase states of monolayers depend on Van der Waals forces and intermolecular interactions between the polar groups of molecules.[16,17]

Isotherms of compression of amphiphilic polybetaines monolayers on the water-air surface are shown on Figure 7. The curves were recorded after 30 min from the moment of spreading of solution onto subphase. It is observed that the π-A isotherms (Figure 7, curve 1) of CROTDA-MAA ($C_{14}H_{29}$) and CROODA-MAA ($C_{18}H_{37}$) are typical for liquid state.[8,15]

Initially the monolayer of amphiphilic polymer is in the gaseous phase (Figure 7, curve 1). It is evidenced by almost unchangeable values of π.[16,26] Starting from $1.3 \pm 0.05\ nm^2 \cdot$monomeric unit^{-1} the surface pressure rises gradually up to $A \approx 0{,}6 \pm 0.05\ nm^2 \cdot$ monomeric unit^{-1} with a collapse pressure at 48 $mN \cdot m^{-1}$. The

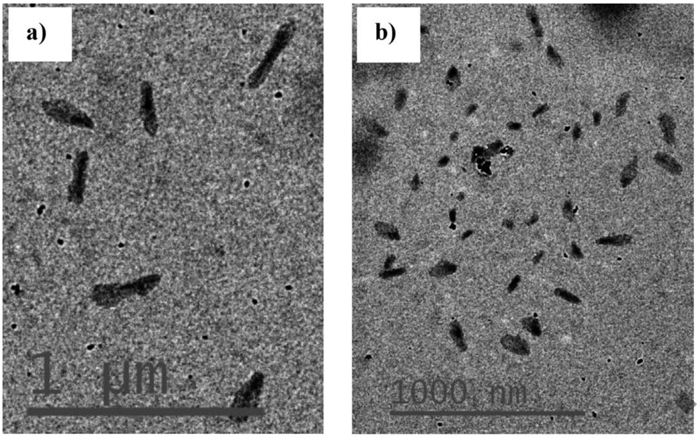

TEM pictures of CROHDA-MAA ($C_{16}H_{31}$) in aqueous KOH solution. C=30 mg/mL

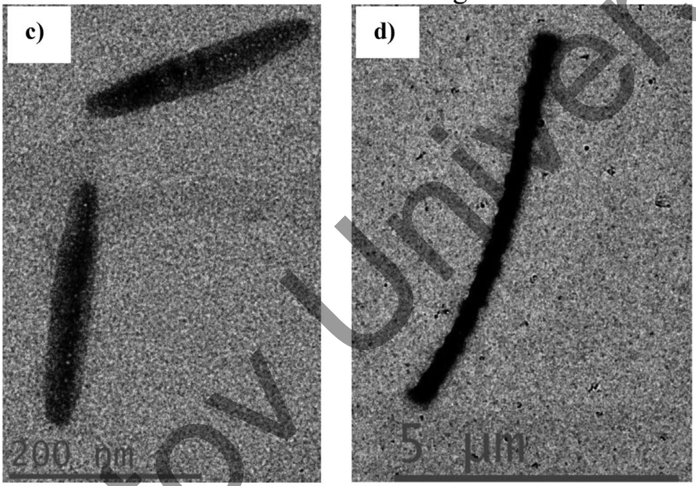

TEM pictures of CROTDA-MAA ($C_{14}H_{29}$) in aqueous KOH solution. C=15 (c) and 45 (d) mg/mL

Figure 5.
TEM pictures of CROHDA-MAA (a, b) and CROTDA-MAA (c, d) in aqueous KOH solution at concentrations of 30 mg/mL (a, b), 15 mg/mL (c) and 45 mg/mL (d).

specific surface area per monomeric unit was estimated by extrapolation of curve 1, Figure 7 on the abscissa axis at defined values of π.

Similarly the π-A curves were obtained for polymer with a longer hydrophobic chain (Figure 7, curve 2). The curve 2 for C18-CROODA-MMA is shifted to the area of small values of A in comparison with curve 1. Monolayer collapses at pressure about $50\,\mathrm{mN} \cdot \mathrm{m}^{-1}$ and the specific surface area is equal to $0.6 \pm 0.05\,\mathrm{nm}^2 \cdot$ monomeric unit^{-1}. Change of solution volume spreaded onto subphase practically not influences on the shape and position of isotherms along to abscissa for both polymers.

The spatial conformation of the monomer unit of CROTDA-MAA was modeled by the MM+ force field method (HyperChem 8). It was found that if the plane of

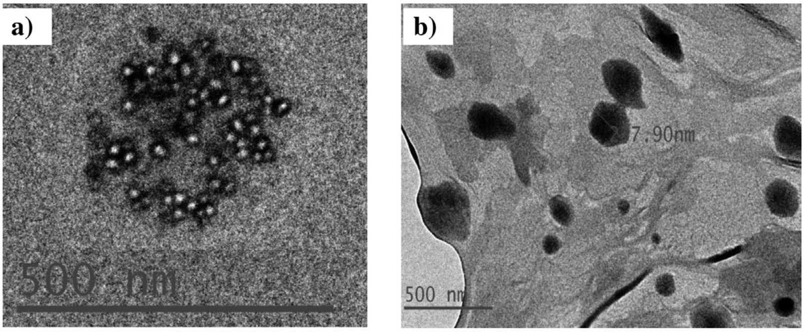

TEM pictures of CROTDA-MAA ($C_{14}H_{29}$) in DMSO. C=7.5 (c) mg/mL

TEM pictures of CROTDA-MAA ($C_{14}H_{29}$) in DMSO. C=15 (c) mg/mL

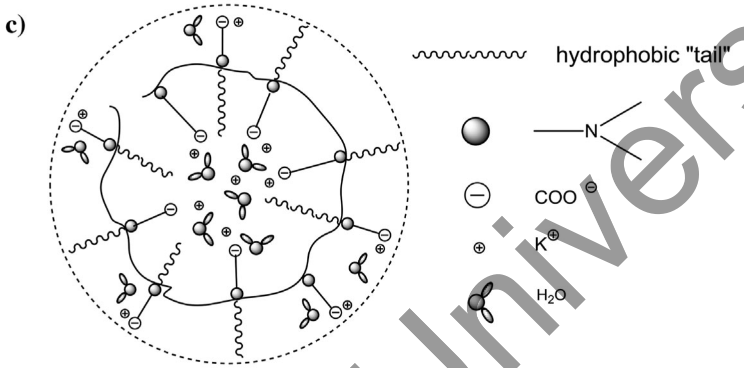

Figure 6.
TEM images of CROTDA ($C_{14}H_{29}$) in DMSO and schematic representation of mixed micelle structure. $C = 7.5\ \text{mg} \cdot \text{mL}^{-1}$.

the betaine groups of polymer chain is located in subphase surface, the specific area A is equal to $0.55 \pm 0.05\ \text{nm}^2 \cdot$ monomeric unit^{-1}, the hydrophobic C14 tail of the CROTDA-MAA is located at the angle approximately 80 degrees to the plane of water surface, as shown in the inset of Figure 7. Such situation is possible when the surface pressure of monolayer is greater than $35\ \text{mN m}^{-1}$. In our experiment the lesser values of A were registered. It can be explained assuming that some parts of hydrophilic monomer unit will be located outside of the subphase.

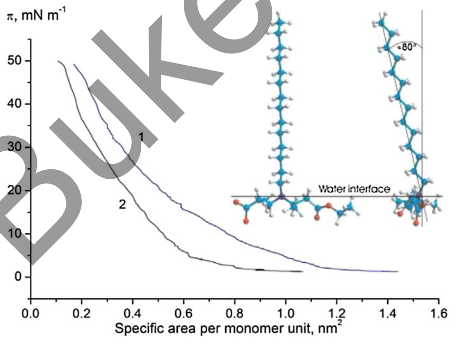

Figure 7.
π-A-isotherms of CROTDA ($C_{14}H_{29}$, V = 0.5 mL) (1) and CROODA ($C_{18}H_{37}$, V = 0.3 mL) (2). In the inset: modeled orientation of CROTDA-MAA monomeric unit on the water-air interface.

To maintain the required density of polymeric monolayers in the course of their transfer onto solid substrate the stability of films was studied by the method of fixation of the changing of surface pressure at constant area of monolayer during 120 minutes.[27,28] In this case the 0.2 mL of polybetaine solution was spreaded onto subphase surface. After 30 min the monolayer was compressed up to $30\ \text{mN} \cdot \text{m}^{-1}$ and the change of π was recorded. The

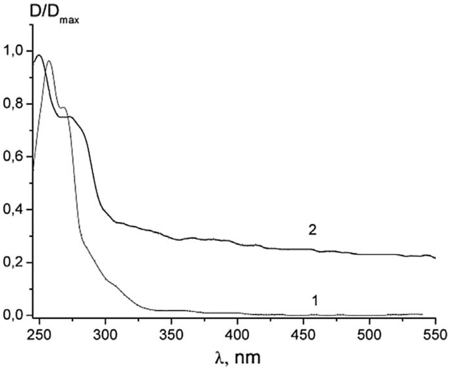

Figure 8.
Normalized absorption spectra of CROTDA-MAA in THF solution (1) and in LB film (2).

surface pressure for both CROTDA-MAA ($C_{14}H_{29}$) and CROODA-MAA ($C_{18}H_{37}$) decreased by $2\,mN \cdot m^{-1}$ during 2 h. The obtained results confirm high stability of polybetaines monolayers. The monolayers were transferred onto quartz substrates by vertical dipping according to Y-type transfer (transfer during downward and upward stroke) at pressure of $\pi = 30$ mN $\cdot$ m^{-1}.

Absorption spectra of $2 \cdot 10^{-4}$ mol $\cdot$ L^{-1} CROTDA-MAA solution in THF together with LB films are shown in Figure 8. The spectra were normalized to maximal D for both curves. It is seen that the absorption band of CROTDA-MAA exhibits the maxima at 255 and 270 nm. In visible range of wavelengths the polymer does not absorb the light. Absorption spectrum of the LB film is broadened in comparison with the spectra of solution. The absorption spectrum of the LB film exhibits a maximum at 250 nm with the shoulder around of 274 nm. For the polymer with $C_{18}H_{37}$ hydrophobic tail (CROODA-MAA) similar absorption spectra were registered because the hydrophobic tails are not involved to the formation of electronic absorption band.[20]

Conclusion

Hydrophobically modified polymeric betaines synthesized from alkylaminocrotonates and methacrylic acid exhibited the polyelectrolyte character in both aqueous and organic solutions. The average hydrodynamic size of macromolecules decreases with dilution due to destruction of big aggregates. The zeta-potential of amphoteric macromolecules in aqueous KOH and DMSO is negative because of presence of ionized carboxylic groups. The isoelectric points (IEP) of amphoteric macromolecules were found to be in the range of pH 2.7–3.4. TEM results revealed the formation of micro- and nanosized micelles, tubular vesicles and rod-like structures in both aqueous KOH solution and DMSO. It is suggested that the big and small vesicles are formed due to inter- and intramacromolecular aggregations of polymer chains stabilized by hydrophobic interactions of long alkyl groups.

The hydrophobic polyampholytes form the stable monolayers on water/air surface. Monolayers with different orientations of the monomers are formed at various surface pressures. It was found that at high surface pressure π the plane of the hydrophilic fragments of polymers is located in parallel plane to the water surface. Increasing in the length of hydrophobic fragments in monomer units leads to the reduction of the specific molecular area in monolayer. The absorption band of CROTDA-MAA in THF solution exhibits the maxima at 255 and 270 nm while LB film has the absorption maximum at 250 and 274 nm.

Thus, the structure of hydrophobically modified polybetaines in liquid and solid media can be changed and controlled by the microenvironment (solvent, pH, concentration) to create objects with predicted structure. The proposed method of deposition of polybetaine monolayers onto a solid substrate can potentially be used to produce the thin films for different applications.

Acknowledgement: Financial support from the Ministry of Education and Science of the Republic of Kazakhstan is greatly acknowledged

(Grant No. 3397/GF4 2015-2017; 1123/GF4 2015-2017; 0088/PCF-14 215–2017).

[1] S. Kudaibergenov, *Polyampholytes: Synthesis, Characterization and Application*, Kluwer Academic Plenum Publishers, New York **2002**. p. 214.

[2] K. Johnson, M. J. Fevola, C. L. McCormick, *J. Appl. Polym. Sci* **2004**, *92*, 647.

[3] S. E. Kudaibergenov, W. Jaeger, A. Laschewsky, *Adv. Polym. Sci.* **2006**, *201*, 147.

[4] I. Dimitrov, B. Trzebicka, A. H. E. Müller, A. Dworak, C. B. Tsvetanov, *Prog. Polym. Sci.* **2007**, *32*, 1275.

[5] A. E. Smith, X. Xu, D. Savin, C. L. McCormick, *Macromolecules* **2010**, *43*, 1210.

[6] A. Takahashi, M. Kawaguchi, *Adv.Polym.Sci.* **1982**, *46*, 1.

[7] G. Garg, Gh. S. Chauhan, R. Gupta, J.-H. Ahn, *J. Colloid Interf. Sci* **2010**, *344*, 90.

[8] N. Hilal, O. O. Ogunbiyi, N. J. Miles, R. Nigmatullin, *Sep. Sci. Technol.* **2005**, *40*, 1957.

[9] B. Van der Bruggen, M. Mänttäri, M. Nyström, *Sep. Purif. Technol.* **2008**, *63*, 251.

[10] J. Sun, F. Zeng, H. Jian, Sh. Wu, *Biomacromolecules* **2013**, *14*, 728.

[11] R. Covis, T. Vives, C. Gaillard, M. Benoi, Th. Benvegnu, *Carbohydr. Polym.* **2015**, *121*, 436.

[12] S. Colak, G. N. Tew, *Biomacromolecules* **2012**, *13*, 1233.

[13] Ch. Leng, K. A. Gibney, Yu. Liu, G. N. Tew, Zh. Chen, *ACS Macro Lett.* **2013**, *2*, 1011.

[14] P. J. Molinoa, G. G. Wallacea, T. W. Hanks, *Synth. Metals* **2012**, *15–16*, 1464.

[15] S. E. Kudaibergenov, Zh. K. Sadakbayeva, G. S. Tatykhanova, N. Medard, A. S. Seitov, Kh. A. Abdullin, *Macromol. Symposia* **2012**, *317–318*, 7.

[16] A. Adamson, *Physical Chemistry of Surfaces*, A Wiley-Interscience Publication, New York **1997**.

[17] A. P. Girard-Egrot, L. J. Blum, in *Langmuir-Blodgett Technique for Synthesis of Biomimetic Lipid Membranes*, D. Martin, Ed., Springer, New York **2007**, p. v.12//23.

[18] D. Martin, *Nanobiotechnology of Biomimetic Membranes*, Springer, New York **2007**. p. 174.

[19] S. A. Yeroshina, N. Kh. Ibrayev, S. E. Kudaibergenov, *Proceed. of SPIE* **2006**, *6263*, 62630E.

[20] S. A. Yeroshina, N. Kh. Ibrayev, S. E. Kudaibergenov, F. Rullens, M. Devillers, A. Laschewsky, *Thin Solid Films* **2008**, *516*, 2109.

[21] S. E. Kudaibergenov, L. A. Bimendina, M. G. Yashkarova, *J. Macromol. Sci. Pure Appl. Chem.* **2007**, *44*, 899.

[22] R. B. Koizhaiganova, S. E. Kudaibergenov, K. E. Geckeler, *Macromol. Rapid Commun.* **2002**, *23*, 1041.

[23] G. Wen, B. Chung, T. Chang, *Polymer* **2006**, *47*, 8575.

[24] L. Chen, T. Chen, W. Fang, Yi. Wen, Sh. Lin, J. Lin, Ch. Cai, *Biomacromolecules* **2013**, *14*, 4320.

[25] R. Enomoto, M. Khimani, P. Bahadur, Sh. Yusa, *J. Taiwan Inst. Chem. Eng.* **2014**, *45*, 3117.

[26] G. Hass, M. H. Francombe, R. W. Hoffman, *Physics of Thin Films*, Academic Press, New York and London **1973**.

[27] V. V. Arslanov, *Uspekhi Khimii (Rus. Chem. Rev.)* **2000**, *10*, 1155.

[28] E. Seliverstova, N. Ibrayev, S. Kudaibergenov, *J. Appl. Polym. Sci.* **2013**, *129*, 289.